Experimental/numerical analysis of the collapse behavior of steel pipes

Andrea P. Assanelli, Rita G. Toscano, Daniel H. Johnson and Eduardo N. Dvorkin
Center for Industrial Research, FUDETEC, Buenos Aires, Argentina

Received October 1999
Revised March 2000
Accepted March 2000

Keywords *Numerical analysis, Steel, Pipes, Pressure, Process control*

Abstract *The production of steel pipes with guaranteed external collapse pressure (e.g. high collapse casings for oil wells) requires the implementation of an accurate process control. To develop that process control it is necessary to investigate how different parameters affect the external collapse pressure of the pipes. Experimental/numerical techniques implemented to investigate the collapse behavior of steel pipes are presented. The discussion of the experimental techniques includes the description of the facilities for performing external pressure collapse tests and the description of an imperfections measuring system. The numerical techniques include 2D and 3D finite element models. The effects on the value of the pipes' external collapse pressure of their shape, residual stresses and material properties are discussed.*

1. Introduction

In many industrial applications it is of great technical and economical importance to have steel pipes with a guaranteed external collapse pressure; for example, the collapse of a casing tube (see Figure 1) inside an oil well usually implies important economical losses for the oil field operator and can also cause a severe environmental accident. Hence, the oil industry is increasingly demanding casing products for which the manufacturers guarantee a minimum performance, which is measured via the external pressure collapse test; those tubular products are known as high collapse casings.

For the reliable production of high collapse casings a stringent process control procedure has to be established. The design of this process control procedure is based on a detailed knowledge of the effect of several factors that can enhance or diminish the external collapse pressure of tubular products, e.g. external surface shape, wall thickness distribution, circumferential residual stresses, etc.

The external collapse pressure of very thin steel pipes is governed by classical elastic buckling formulas (Timoshenko and Gere, 1961; Brush and Almroth, 1975); however, for thicker pipes more involved elasto-plastic considerations have to be taken into account. There are many factors that have some degree of influence on the external pressure that produces the collapse of a steel pipe, among them (Heise and Esztergar, 1970; Clinedinst, 1977; Tomita and Shindo, 1982; Fowler *et al.*, 1983; Krug, 1983; Kanda *et al.*, 1983; Mimura *et al.*, 1987):

The authors acknowledge the financial support for this research from SIDERCA (Campana, Argentina) and TAMSA (Veracruz, Mexico).

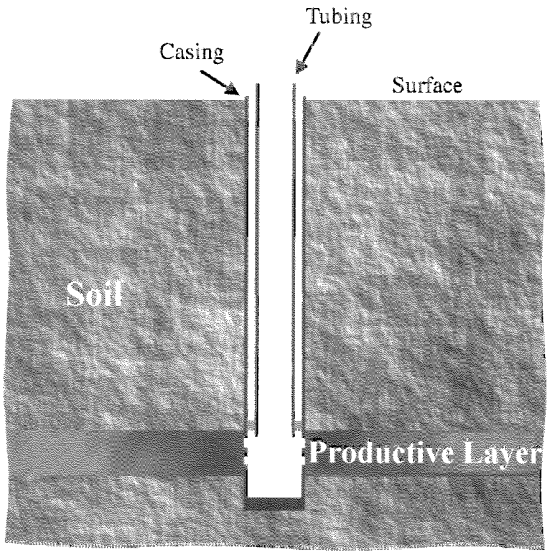

Figure 1.
Steel tubes (casing and tubing) in an oil well

- The relation (outside diameter/thickness) (D/t ratio).
- The yield stress of the pipe steel (σ_y).
- The work-hardening of the pipe steel.
- The geometry of the pipe (outside diameter shape and wall thickness distribution).
- The circumferential residual stresses in the pipe steel.
- The localized imperfections in the pipe body.

For steel pipe manufacturers it is very important to quantify the effect of the above listed variables when establishing the specifications for their products and when designing their processes to meet those specifications. While there is a general agreement on the effects of (D/t) and σ_y on the collapse pressure, as expressed, for example, in the API calculation formulas (Bull. 5C3, 1994), the effect of the other factors is still the subject of many research efforts.

In this paper we present the experimental techniques and the hierarchy of finite element models that we have developed to study the collapse behavior of steel pipes.

In section 2 we comment on our facilities for performing external pressure collapse tests and we also present an imperfections measuring system that we have implemented at our laboratory based on the device described in Yeh and Kyriakides (1988) (see also Arbocz and Babcock (1969) and Arbocz and Williams (1977)).

In section 3 we present the 2D finite element models that we have developed, as a first approach, for the simulation of the external pressure collapse test. We compare the collapse pressures predicted by these 2D models with the

experimental results obtained at our laboratory; the comparison demonstrates that a 2D geometrical characterization of the pipes cannot guarantee a very accurate prediction of the collapse pressure of actual pipes. However, the 2D models are a useful tool for performing parametric studies on the effects of the pipes' ovality, eccentricity, circumferential residual stresses and work-hardening on the external collapse pressure value.

The pipe shape imperfections and the wall thickness normally change along the pipe length; also localized imperfections can be found in the pipes. In section 4 we present the 3D finite element models that we have developed to overcome the limitations of the simpler 2D models.

The 3D model predictions have been qualified via experimental testing at our laboratory; the geometrical information on the tested samples has been acquired using our imperfections measuring system and has been used as data for the 3D finite element models.

In section 5 we analyze, using our experimental results, the accuracy of an empirical formula that was developed to predict the external collapse pressure of steel pipes (Tamano *et al.*, 1983). Since the empirical formula uses only a 2D geometrical characterization of the pipes' geometry, it is equivalent to the 2D finite element models regarding the accuracy of its predictions (section 3).

2. Experimental procedures

In the present section we describe our laboratory facilities for performing external pressure collapse tests and we also present the imperfections measuring system that we have developed based on Yeh and Kyriakides (1988), Arbocz and Babcock (1969) and Arbocz and Williams (1977).

2.1 External pressure collapse tests

A schematic drawing of the pressure vessels used in our lab for performing external pressure collapse tests is shown in Figure 2. It is important to notice that:

- The experimental set-up does not impose axial restraints on the pipes (Bull. 5C3, 1994);
- The length of the sample being tested fulfils in all cases the relation: $(L/D) > 10$ (Fowler *et al.*, 1983).
- The collapse of the samples is detected by a drop in the pressure of the water used to pressurize them.
- The chamber can be moved to a testing frame to add axial load and/or constant bending to the sample.

2.2 Imperfections measuring system

In order to acquire information on the geometry of the pipe samples that are going to be tested in the collapse chamber, the shape of the external surface is mapped and the wall thickness is measured at a number of points.

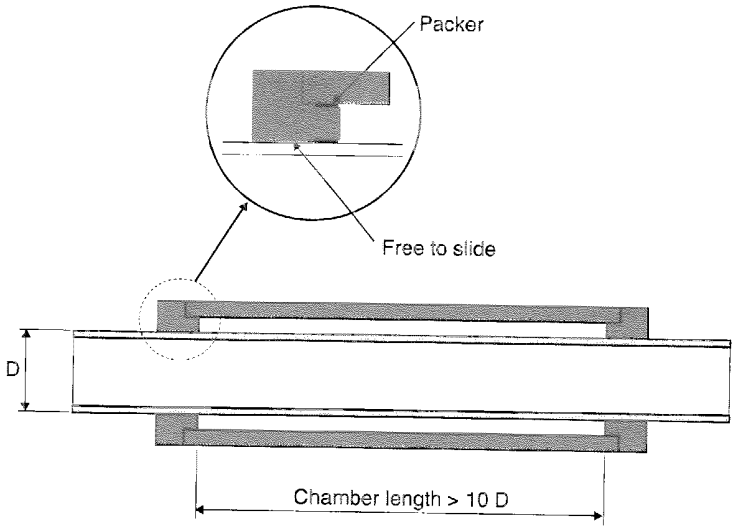

Figure 2.
Collapse chamber

2.2.1 Mapping of the sample's external surface. To map the external surface of a sample we rotate it in a lathe and at regular intervals of time, radial and angular positions are sent to an acquisition system. The position of the pipe surface is recorded from a linear variable displacement transducer (LVDT (see Figure 3)). A rotary encoder placed on the rotation axis provides the angular position. We have developed an algorithm to transform the acquired data into the Fourier series description of the sample's external surface (see Appendix).

In Figure 4 (a-c) we present the Fourier decomposition obtained using the above described algorithm in the case of the following three tubular samples:

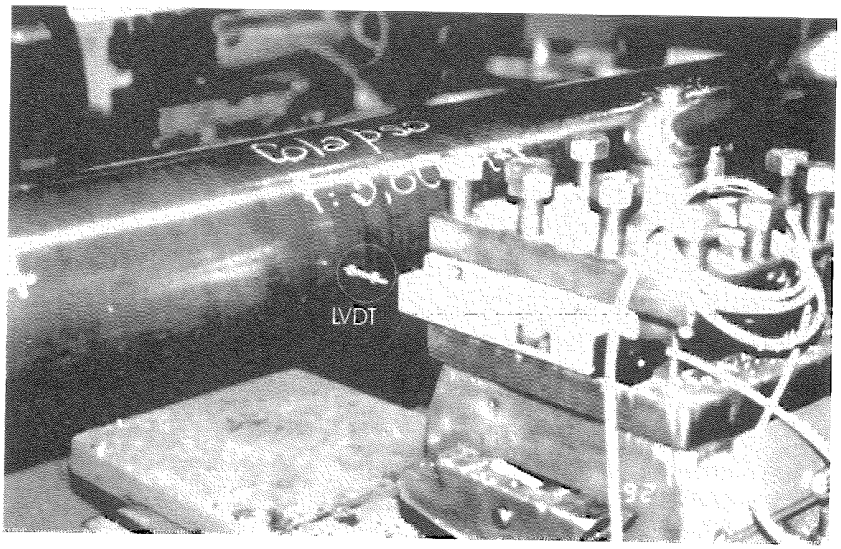

Figure 3.
Mapping of the sample's external surface

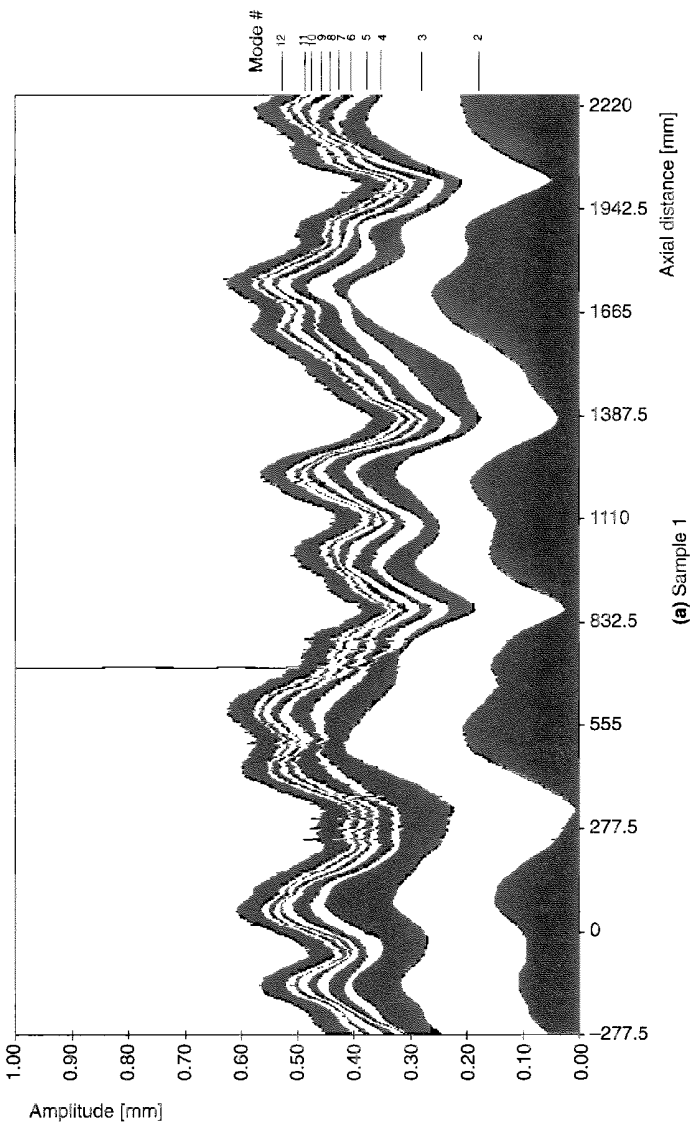

Figure 4a.
External surface Fourier decomposition. Sample 1

(1) Sample 1: $9\frac{5}{8}$" nominal outside diameter with a metric weight of 47lb/ft – Grade 95 (minimum yield stress: 95Ksi (655MPa); maximum yield stress: 125Ksi (862MPa)).

(2) Sample 2: 7" nominal outside diameter with a metric weight of 23lb/ft – Grade 95.

(3) Sample 3: 7" nominal outside diameter with a metric weight of 26lb/ft – Grade 95.

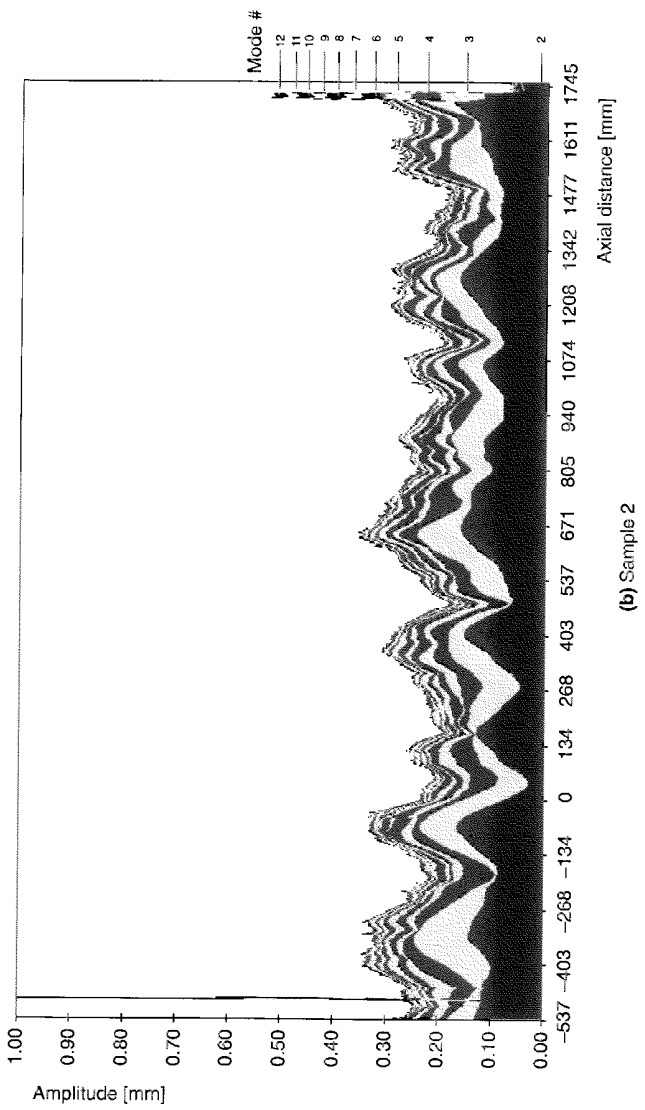

Figure 4b.
External surface Fourier decomposition. Sample 2

The length of each sample is approximately 3m, the pitch of the cross-slide is 3.7mm/turn and the angular distance between the acquired points is one degree.

The above samples correspond to heat treated pipes that were produced using the following rolling facilities: retained mandrel mill with two rolls/stand and sizing mill with three rolls/stand. It is interesting to notice, in Figure 4, that the most relevant imperfection amplitudes correspond to the second mode (oval shape) and third mode (triangular shape).

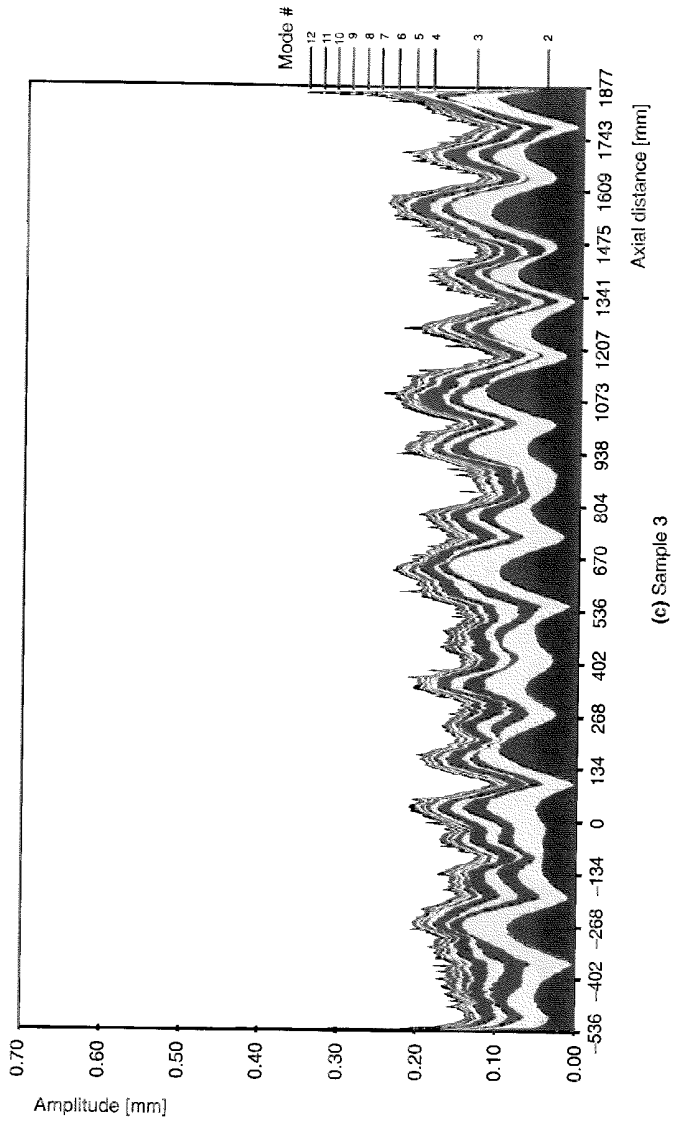

Figure 4c.
External surface Fourier decomposition. Sample 3

2.2.2 Wall thickness measurement. We measure the wall thickness at a number of points evenly distributed on the sample external surface, using manual ultrasonic gauges; the thickness maps of the measured samples are represented in Figure 5.

3. Two-dimensional finite element models

In this section we discuss the 2D finite element models that we have implemented to simulate the behavior of ideal long specimens in the external

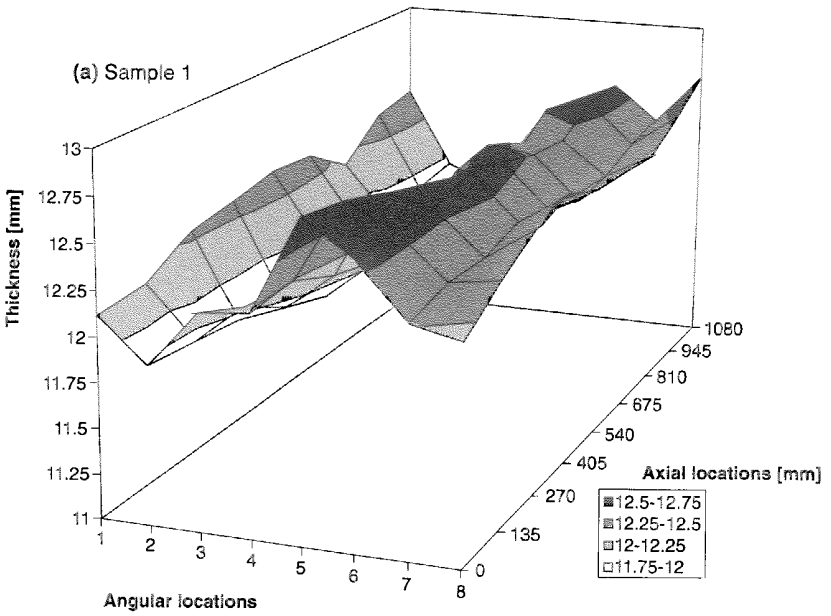

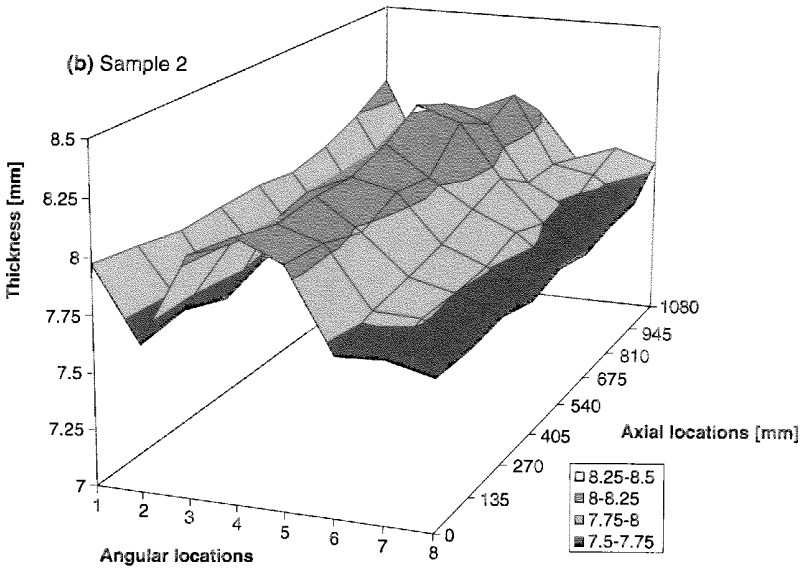

Figure 5.
Thickness measurements (*continued*)

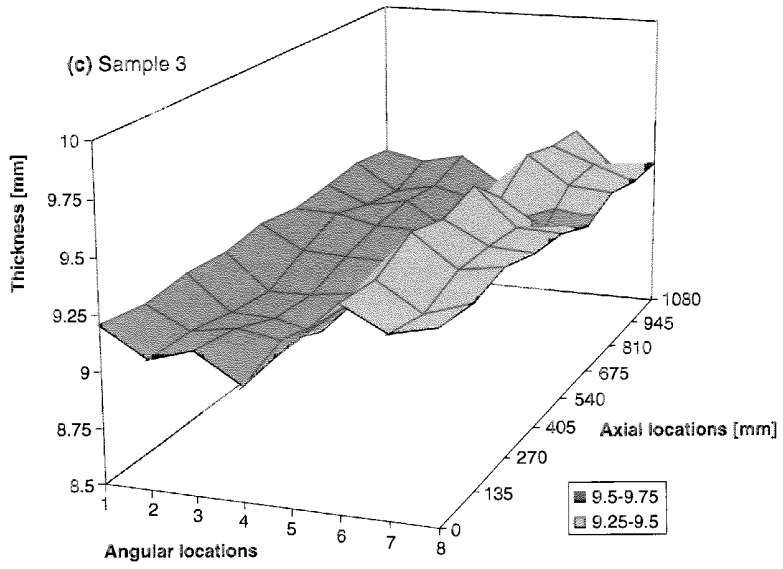

Figure 5.

pressure collapse test. We also compare experimental results with the predictions of these 2D models: the comparison demonstrates that a 2D geometrical characterization of the pipes does not contain enough information to assess their collapse strength. However, the 2D models can provide useful information on the trends of the external collapse pressure value when some parameters – such as circumferential residual stresses, shape imperfections, etc. – are changed.

3.1 Formulation of the 2D models

We develop the 2D finite element models using a total Lagrangian formulation (Bathe, 1996) that incorporates:

- Geometrical non-linearities due to large displacements/rotations (infinitesimal strains assumption).
- Material non-linearity: an elasto-plastic constitutive relation is used for modeling the steel mechanical behavior (Von Mises associated plasticity (Hill, 1971)).

We carry out the finite element analyses using the general purpose finite element code ADINA (*ADINA Users' Manual,* 1996) in which we incorporated the quadrilateral QMITC element as a "user defined element" (Dvorkin and Vassolo, 1989; Dvorkin and Assanelli, 1989; Dvorkin *et al.,* 1996).

For modeling the external hydrostatic pressure we use follower loads (Brush and Almroth, 1975), and we introduce in our models the circumferential residual stresses with a linear distribution across the thickness.

In our laboratory we use the classical slit-ring test for measuring the circumferential residual stresses in the pipe samples (Marlow, 1982; Tamano *et al.*, 1983; Krug, 1983). In order to validate our procedure for simulating the circumferential residual stresses, in Figure 6 we present the result of the 2D finite element simulation of a slit-ring test; the slit process was simulated eliminating a row of elements. The model results agree with our experimental observations; hence we can consider that our circumferential residual stresses simulation is realistic enough.

When using a 2D model it is important to recognize that the actual collapse test is not modeled exactly either by plane strain or by plane stress models because:

(1) The absence of longitudinal restraints imposes a plane stress situation at the sample edges.

(2) The length of the samples ($L/D > 10$) approximates a plane strain situation at its center.

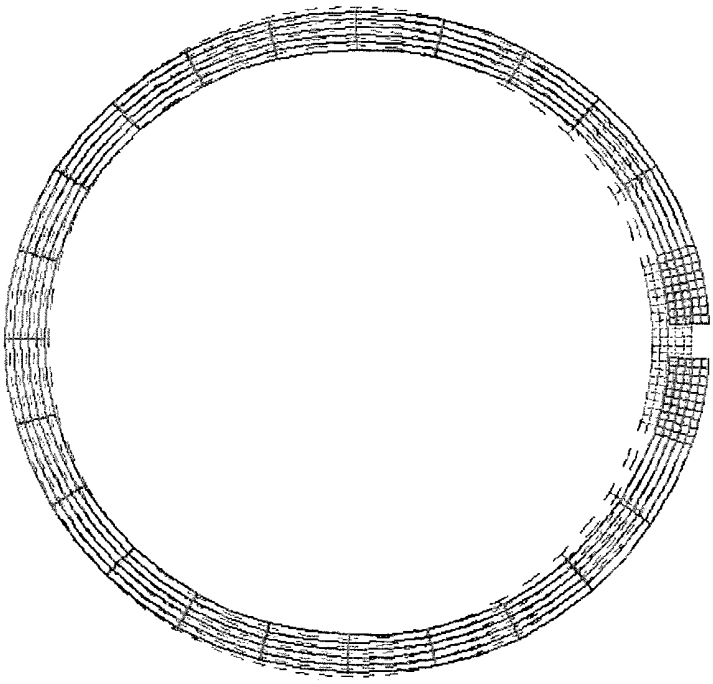

Figure 6.
Two-dimensional simulation of the slit-ring test

In section 4 when presenting the results that we obtain using 3D models we will return to this discussion. In this section, however, in order to explore the limitations of the 2D models we analyze the collapse test using both plane stress and plane strain finite element models.

3.2 Two-dimensional finite element results vs. experimental results

The 2D finite element models have been developed considering an elastic-perfectly plastic material constitutive relation. We will show in section 3.3 that disregarding the steel work-hardening introduces only a negligible error in the calculated collapse pressures.

For standard samples in which the pipe geometry is not analyzed using the above described imperfections measuring system, the laboratory keeps records of the following geometrical parameters:

- average, maximum and minimum outside diameter at three sections (the central section and the two end sections);
- thicknesses at the two end sections (eight points per section).

We construct the geometry of the 2D finite element models using:

- the ovality (Ov) and the average outside diameter of the central section;
- the eccentricity (ϵ) obtained by averaging the eccentricities of the two end sections;
- the thickness obtained by averaging all the thickness determinations.

The ovality and eccentricity are defined as:

$$Ov = \frac{D_{max} - D_{min}}{D_{average}} \quad ; \quad \epsilon = \frac{t_{max} - t_{min}}{t_{average}} \tag{1}$$

The circumferential residual stresses for each sample are measured using a slit-ring test and its values are imposed on the model with a linear distribution through the thickness. The actual transversal yield stress of the sample material is measured and its value is used for the elastic-perfectly plastic material constitutive relation.

To determine the collapse loads of the sample models we calculate the non-linear load/displacement path and seek its horizontal tangent.

To perform the numerical analyses we use a 2D mesh with 720 QMITC elements and 1,572 d.o.f. (see Figure 7a). Half of the pipe is modeled due to symmetry. To assess the quality of this mesh we analyze the plane strain collapse of an infinite pipe and we compare, in Table I, our numerical results against the analytical results obtained using the formulas in Timoshenko and Gere (1961).

From the results in Table I we conclude that the proposed 2D mesh of QMITC elements is accurate enough to represent the collapse of very long specimens.

From the analyses of different cases we have identified two basic types of load/displacement paths:

(1) In Figure 7b we present the load/displacement path of an eccentric pipe with ($D/T = 22.13$).

(2) In Figure 7c we present the load/displacement path of another eccentric pipe but with ($D/t = 17.67$).

The second case presents an inverse collapse behavior that was previously described in Corona and Kyriakides (1987), Fowler *et al.* (1990) for the case of collapse under external pressure and bending.

A total of 32 collapse tests, for pipes $9\frac{5}{8}$" nominal outside diameter with a metric weight of 47lb/ft and 7" nominal outside diameter with a metric weight of 26lb/ft, both Grade 95, have been analyzed using plane stress and plane strain models. The comparisons between the numerical and experimental results are plotted in Figure 8a (plane stress models) and Figure 8b (plane strain models).

Average OD [mm]	245.42
Average thickness [mm]	12.61
D/t	19.47
Ov	0.18%
σ_y [MPa]	890
p_{cr} (Timoshenko and Gere, 1961)/p_{cr} FEA	0.992

Table I.
Qualification of the 2D finite element model

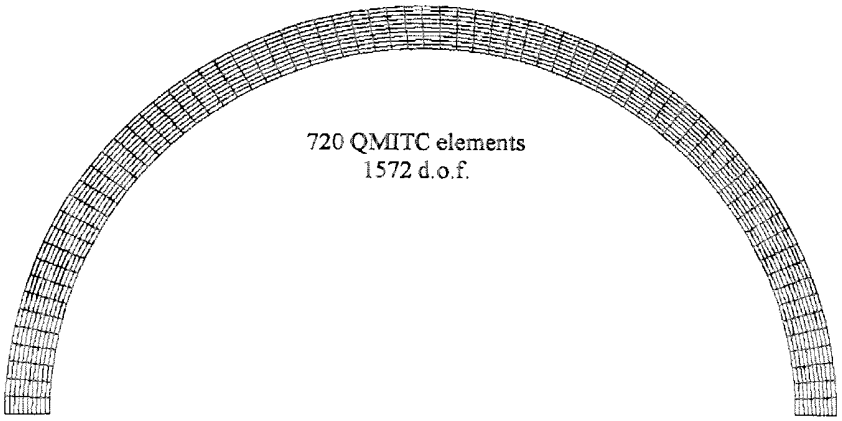

a) 2D finite element mesh

Figure 7.
2D models of the external pressure collapse test
(continued)

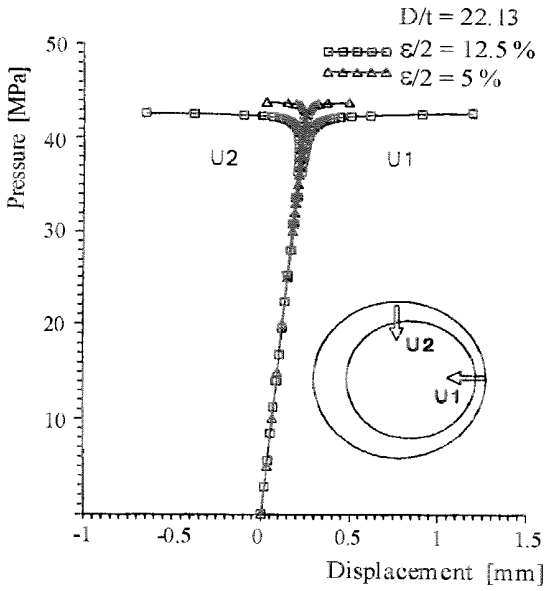

b) Eccentric tube: direct collapse behavior

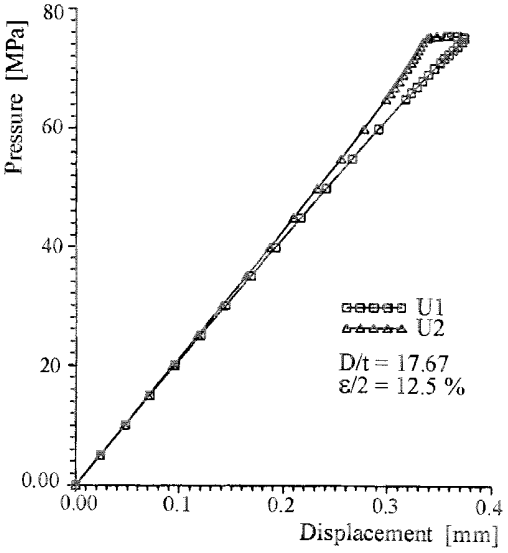

c) Eccentric tube: inverse collapse behavior

Figure 7.

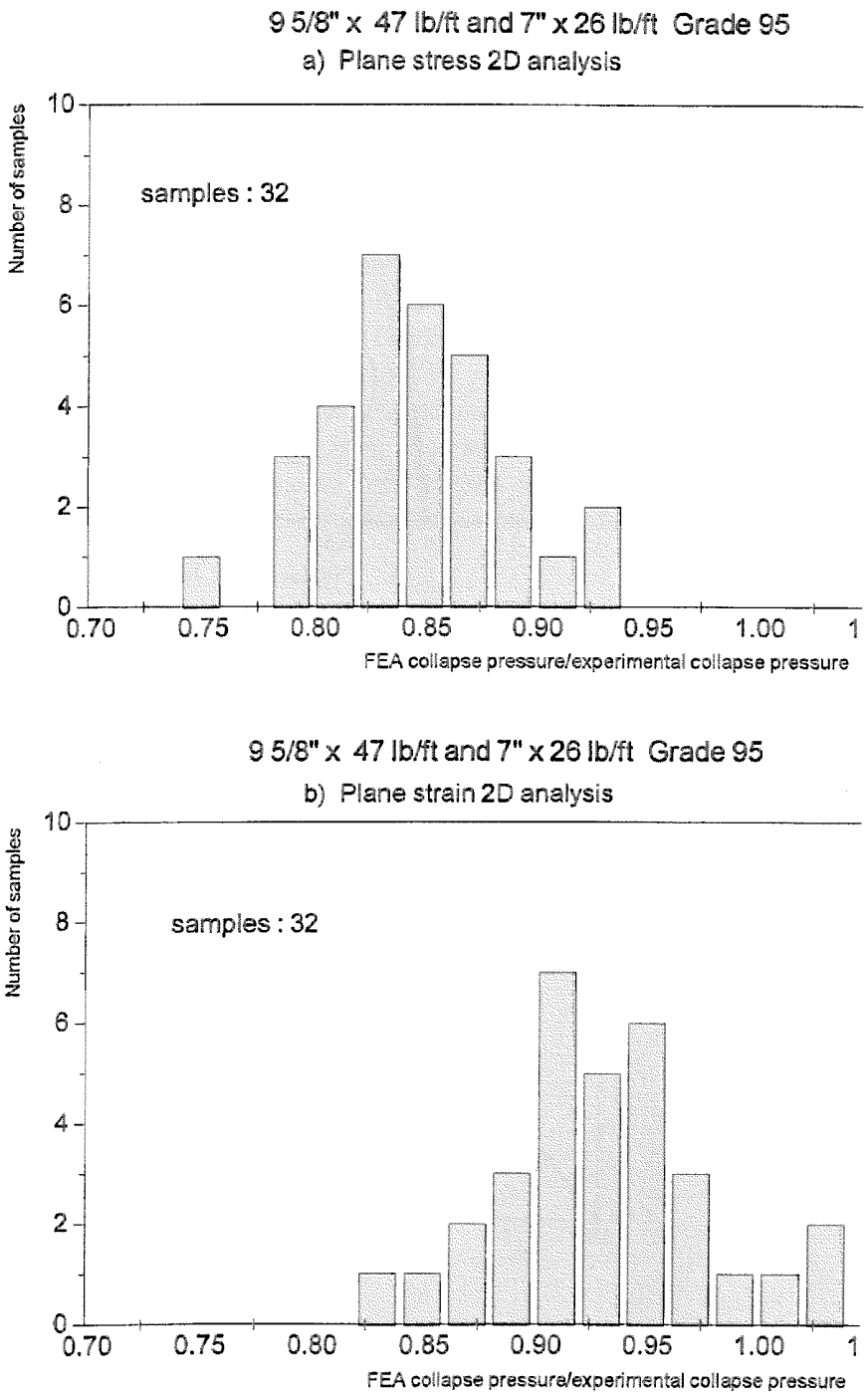

Figure 8.
Qualification of the 2D models

It is important to observe that the collapse pressure values determined using the 2D models present a significant deviation from the experimental ones, being in general the former lower than the latter. Some reasons for this behavior are:

- The middle section ovality is not fully representative of the sample geometry (this point explains the disagreement between numerical and experimental results but cannot explain the fact that the numerically determined values are in general lower than the actual ones).
- In developing the 2D models the measured ovality is entirely assigned to the first elastic buckling mode. This conservative approach partially accounts for the fact that the numerical values are lower than the actual ones.
- The experimental set-up (see Figure 2) imposes on the samples unilateral radial restraints at both ends. These restraints are not described by the 2D models; the difference between the numerical and actual boundary conditions also partially accounts for the fact that the collapse pressures predicted by the 2D models are in general lower than the actual ones.

The numerical/experimental technique to be presented in section 4, that combines our imperfections measuring system and 3D finite element models, will remove the above sources of disagreement between numerical and experimental results.

It is obvious, from the results in Figure 8, that the 2D geometrical characterization of a pipe is not enough for performing a very accurate assessment on its collapse performance. However, the 2D models are very useful for performing parametric studies on the relative weight of different factors that affect the external collapse pressure.

3.3 Strain hardening effect

We have previously mentioned that the strain hardening of the pipe material does not play an important role in the determination of its external collapse pressure. In this section we examine the above remark using 2D finite element models.

We analyze two $9\frac{5}{8}$" nominal outside diameter pipes (a thin and a thick one) using a bilinear material model. In order to explore different hardenings we consider three values for the constant plastic tangential modulus:

$$E_T = 0.0(\text{perfect plasticity}) \quad ; \quad 0.057\,E \quad ; \quad 0.10\,\text{E}$$

where E is the Young's modulus. We also consider two ovality (Ov) values but we do not include in this analysis either the pipe eccentricity or its circumferential residual stresses. We summarize the numerical results of our analyses in Table II.

As can be seen, for all the analyzed cases, the strain hardening has a negligible effect on the external collapse pressure value.

It is important to recognize that in the above analyses we have considered σ_y to be independent of E_T. This is not the case if as yield stress we adopt the one corresponding to a relatively large permanent offset (Tokimasa and Tanaka n.d.).

3.4 Effect of ovality, eccentricity and circumferential residual stresses

Using 2D finite element models we develop in this section a parametric study aimed at the analysis of the effect, on the pipes' external collapse pressure, of the following parameters:

- ovality (Ov);
- eccentricity (ϵ);
- circumferential residual stresses (σ_R)

In the present analyses the ovality is considered to be concentrated in the shape corresponding to the first elastic buckling mode and the eccentricity is modeled considering non-coincident OD and ID centers.

In Figure 9 we plot the results of our parametric study, normalized with the collapse pressure calculated according to the API formulas (Bull. 5C3, 1994). It is obvious from these results that the main influence on the external collapse pressure comes from the ovality and from the circumferential residual stresses; however, the effect of the circumferential residual stresses diminishes when the ratio (D/t) evolves from the plastic collapse range to the elastic collapse range. The eccentricity effect, in the case of the external collapse test with neither axial nor bending loads, is minor.

As a conclusion of the above parametric study we can assess that for producing pipe with enhanced collapse pressure it is very important to have both a low ovality and low circumferential residual stresses.

4. Three-dimensional finite element models

In this section we discuss the 3D finite element models that we have implemented to simulate the external pressure collapse test. We use the 3D models with the geometrical data acquired with our imperfections measuring system, described in section 2, and we compare the numerical collapse pressure predictions with the experimental determinations carried out at our laboratory. Afterwards we also use the 3D models to perform some parametric studies.

Table II. Analysis of the work-hardening effect on the external collapse pressure

D/t	Ov [%]	pc ($E_T = 0.0$) [MPa]	pc ($E_T = 0.057E$) [MPa]	pc ($E_T = 0.10E$) [MPa]
17.66	0.75	59.9	60.2	60.4
17.66	0.35	67.1	67.3	67.5
24.37	0.75	26.7	26.7	26.7
24.37	0.35	29.0	29.1	29.1

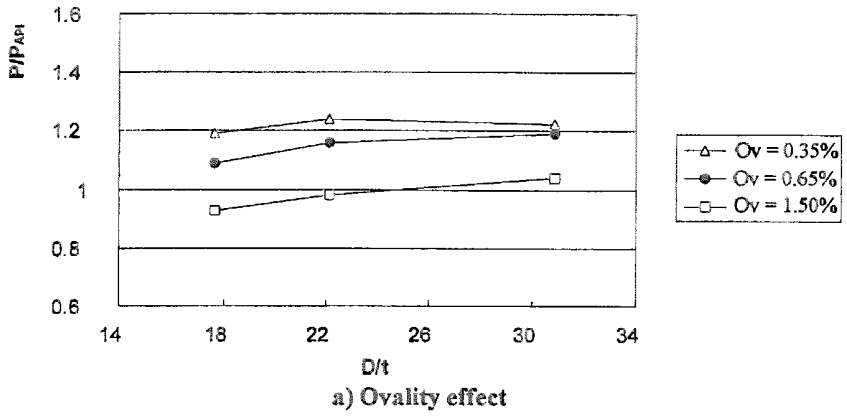

a) Ovality effect

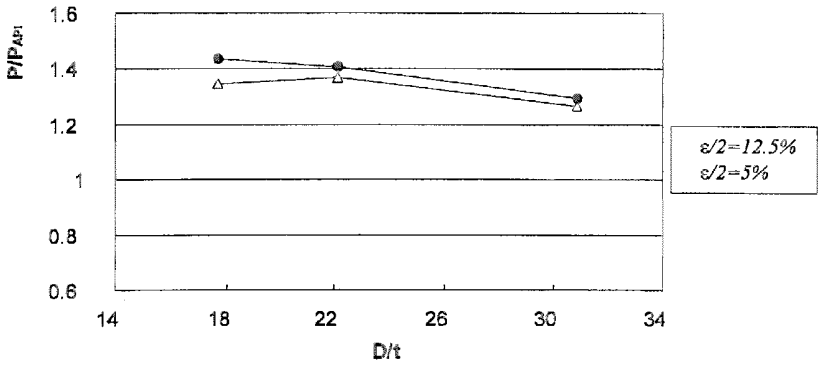

b) Eccentricity effect

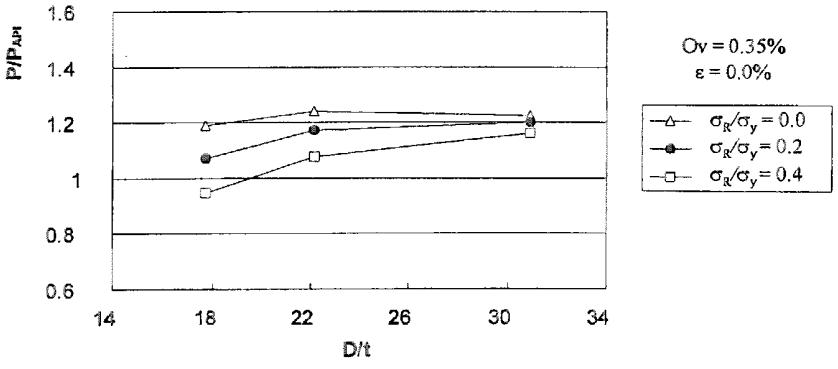

c) Residual stresses effect

Figure 9.
Parametric study of the effect of ovality, eccentricity and residual stresses on the casing collapse pressure. Performed using 2D finite element models

4.1 Formulation of the 3D models

The (radius/thickness) relation of the pipes to be analyzed ranges from 7.61 to 12.08; hence a shell model that incorporates shear deformations is a suitable one. Following what we did for the 2D models we use a total Lagrangian formulation (Bathe, 1996) that incorporates the geometrical non-linearities coming from the large displacements/rotations and the material non-linearity coming from the elasto-plastic constitutive relation. We carry out the finite element analyses using the code ADINA (*ADINA Users' Manual*, 1996) and the MITC4 shell element (Dvorkin and Bathe, 1984; Bathe and Dvorkin, 1985, 1986). As in the previous section, follower loads are used to model the hydrostatic external pressure and the circumferential residual stresses are modeled with a linear distribution through the thickness.

4.2 Circumferential residual stresses

As we see in Figure 9, the correct measurement of the circumferential residual stresses, via the slit-ring test, is fundamental for determining the external collapse pressure of a pipe. In our laboratory we use slit-ring samples with ($L/D = 3$)

To check the capability of our 3D finite element models to simulate different circumferential residual stress patterns we consider a $9\frac{5}{8}$" nominal outside diameter pipe with a metric weight of 47lb/ft – Grade 110 (minimum yield stress: 110Ksi (758MPa); maximum yield stress: 140Ksi (965MPa)). We consider for our example: $\sigma_y = 758\text{MPa}$ and $\sigma_R = 0.2\sigma_y$.

We calculate the value of the sample's opening, in a slit-ring-test, using two different calculation procedures:

(1) Using the analytical relation between the circumferential residual stresses (σ_R) and sample openings (a). For a sample with (L/D) = 3 we use a plane strain formula:

$$a = \frac{4\,\pi\,R^2\,(1-\nu^2)\,\sigma_R}{t\,E} \tag{2}$$

t : average sample thickness;

E : Young's modulus;

R : average sample mid-radius;

ν : Poisson's ratio.

In the above formula we have assumed that the circumferential residual stresses have a linear distribution through the pipe thickness.

(2) Using the 3D finite element model shown in Figure 10, where the circumferential residual stresses are simulated with a linear distribution across the thickness and the slit of the cylindrical sample is simulated by removing a row of elements.

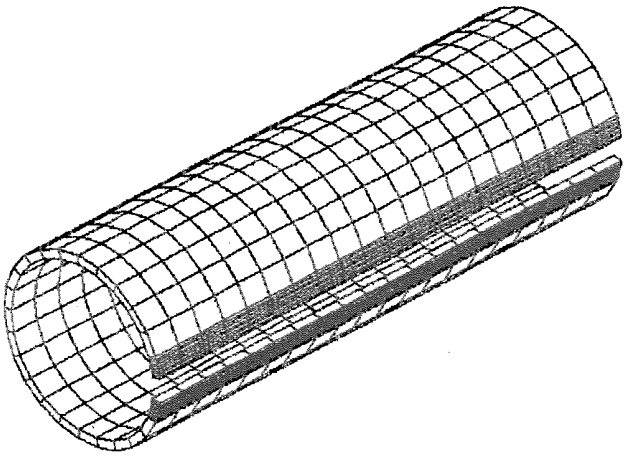

a) After slitting. Lateral view

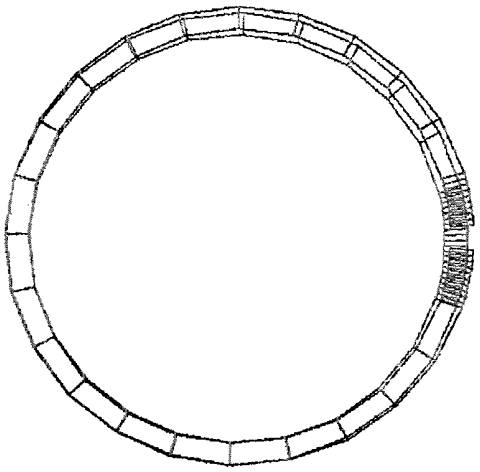

b) Before and after slitting. Front view

Figure 10.
Three-dimensional finite element simulation of the slit-ring test

The relation between the finite element and analytical predicted openings is 0.99; hence our 3D finite element procedure for representing the circumferential residual stresses can be considered realistic enough.

4.3 Three-dimensional simulation of the external pressure collapse test
In order to validate our 3D finite element models of the external pressure collapse test, we analyze the three tubular samples described in section 2 (see Figures 4 and 5). The meshes are generated using only the first 12 modes (see Figure 11) from the external surface Fourier decomposition.

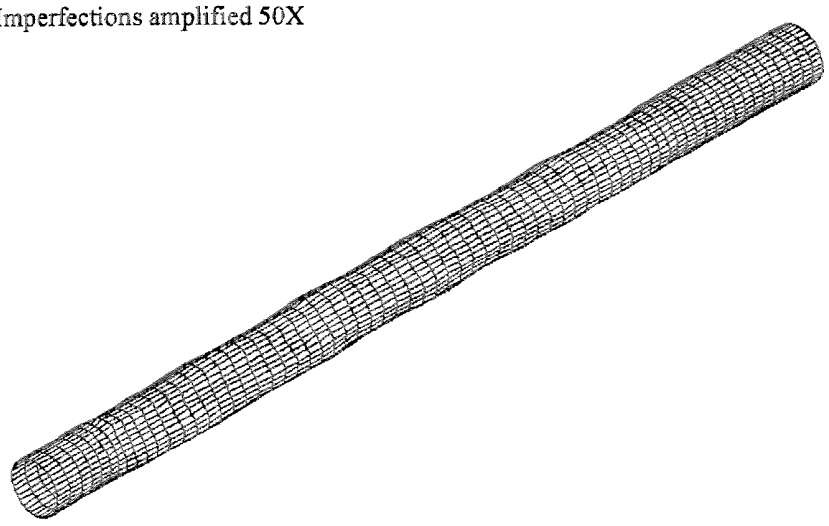

a) Lateral view

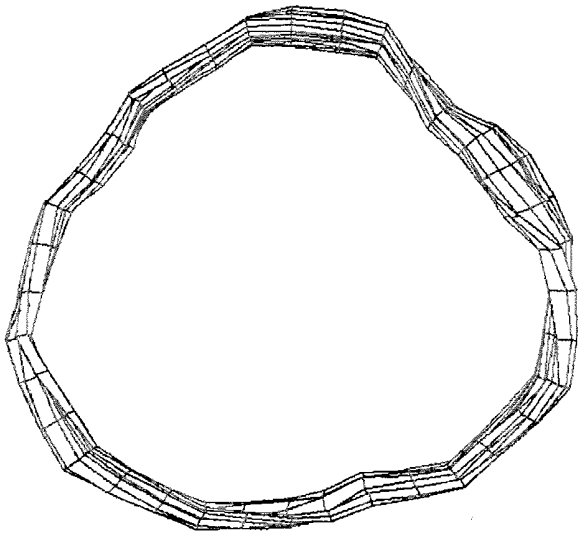

b) Front view

Figure 11.
Finite element mesh developed considering the first 12 modes (sample #1)

The actual transversal yield stress of the samples and the circumferential residual stresses measured using slit-ring samples are shown in Table III.

We analyzed only three cases and the comparison between the finite element determined collapse pressures and the experimentally measured ones is presented in Table IV.

From these results it is evident that the developed 3D finite element models simulate very accurately the external pressure collapse test.

In Figure 12 we plot the axial stresses developed in the samples when the external pressure reaches the collapse value; these axial stresses are maximum at the sample center and zero close to the sample edges (see in section 3.1 the discussion on 2D plane stress and plane strain models).

Sample	D/t	$\sigma_y[MPa]$	σ_R/σ_y
1	16.7	845	0.17
2	22.7	791	0.38
3	19.0	831	0.27

Table III. Mechanical properties of the three analyzed samples

Sample	p_{cr} FEA/ p_{cr} exp
1	1.005
2	1.017
3	0.984

Table IV. Comparison between 3D FEA and experimentally determined collapse pressures

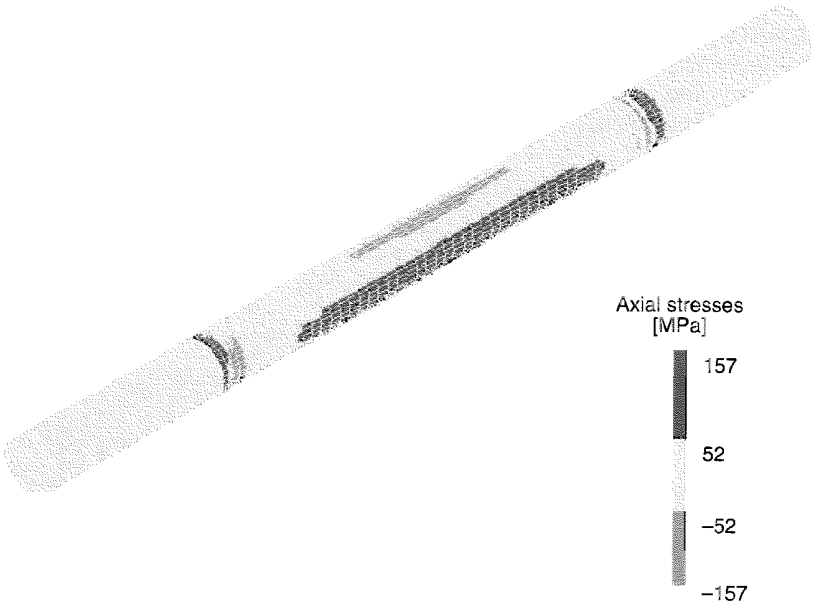

Figure 12. Axial stresses developed when the external pressure reaches the collapse value

4.4 Parametric studies using the 3D model

4.4.1 Effect of low and high shape modes. The numerically calculated values of external collapse pressure that we report in Table IV have been calculated considering 12 shape modes in the external surface Fourier decomposition (see Figure 4). In order to investigate the effect of the different shape modes we re-calculate the collapse pressures but considering only the first four modes (see Figure 4). The numerical results obtained indicate that for the three analyzed cases:

$$p_{cr}^{4modes} = p_{cr}^{12modes} \tag{3}$$

Hence, we may assess that the external collapse pressure value is determined only by the first modes of the external surface Fourier decomposition.

4.4.2 Effect of the shape mode phase angles. In Figure 4 we have plotted for each shape mode its amplitude, as a function of the axial position along the pipe length. However, for every section each mode is described by its amplitude and its phase angle, also variable along the sample length.

In order to investigate the phase angle effect we analyze, using 3D finite element models, an ideal pipe 7" nominal outside diameter pipe with a metric weight of 26lbs/ft – Grade 110. We consider σ_y = 758MPa, a constant nominal thickness and an external surface imperfection corresponding to the second shape mode with Ov = 0.3 per cent. We consider three different values of Θ (twisting over 1.70m in Figure 13); the finite element determined non-linear load paths are shown in Figure 14, and from them we obtain the results presented in Table V.

From the results in Table V it can be observed that the more "twisted" the sample, the higher its external collapse pressure. This is an effect that obviously requires a 3D model to describe it.

5. Qualification of an empirical formula

Based on experimental tests and numerical studies an empirical formula for determining the external collapse pressure value for seamless tubes was proposed (Tamano *et al.*, 1983),

$$p_{cr} = \frac{1}{2}\,(p_{eo} + p_{go}) - \sqrt{0.25\,(p_{eo} - p_{go})^2 + p_{eo}\,p_{go}\,H} \tag{4}$$

where

$$p_{eo} = \frac{2\,E}{(1-\upsilon^2)\,(D/t)\,[(D/t)-1]^2}$$

$$p_{go} = 2\,\sigma_{yz}\,\frac{\sigma_{y\theta}}{\sigma_{yz}}\,\frac{[(D/t)-1]}{(D/t)^2}\left[1 + \frac{1.47}{[(D/t)-1]}\right]$$

$$H = 0.0808\,(100\,Ov) + 0.00114\,(100\,\epsilon) - 0.1412\,s$$

$$s = \frac{\sigma_{R\theta}}{\sigma_{y\theta}}$$

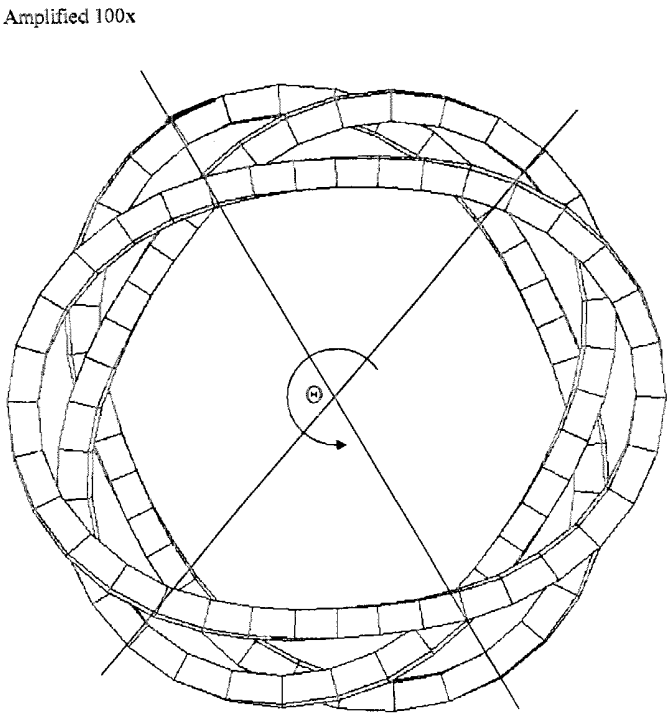

Figure 13.
Twisting angle of the second mode shape

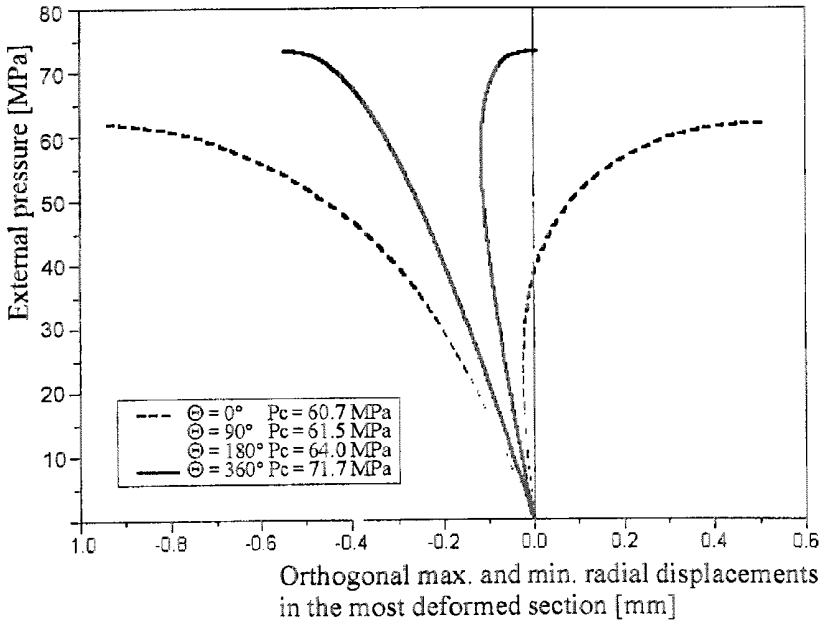

Figure 14.
Effect of the shape mode phase angle on the external collapse pressure

$\sigma_{R\theta}$: circumferential residual stress measured with the slit-ring method (the sign corresponds to the circumferential residual stress in the pipe entrances);

$\sigma_{y\theta}$: yield stress in the hoop direction;

σ_{yz} : yield stress in the longitudinal direction.

This empirical formula uses a constant value for the pipe ovality and eccentricity; in this sense it has the same limitations encountered in the 2D finite element models, to represent three-dimensional geometries. However, the above mentioned formula incorporates empirical parameters that have been determined to minimize the formula prediction errors over a certain set of samples.

We analyze using the empirical formula the 32 tests that were considered in section 3.2, using 2D finite element models.

The comparison between the formula predictions and the experimental results is plotted in Figure 15. It can be observed that the dispersion is quite similar to the dispersion of the 2D FEA models (see Figure 8).

Θ[°/1.7m]	$p_{cr}\|\Theta/p_{cr}\|0°$
90	1.01
180	1.05
360	1.18

Table V.
Phase angle effect

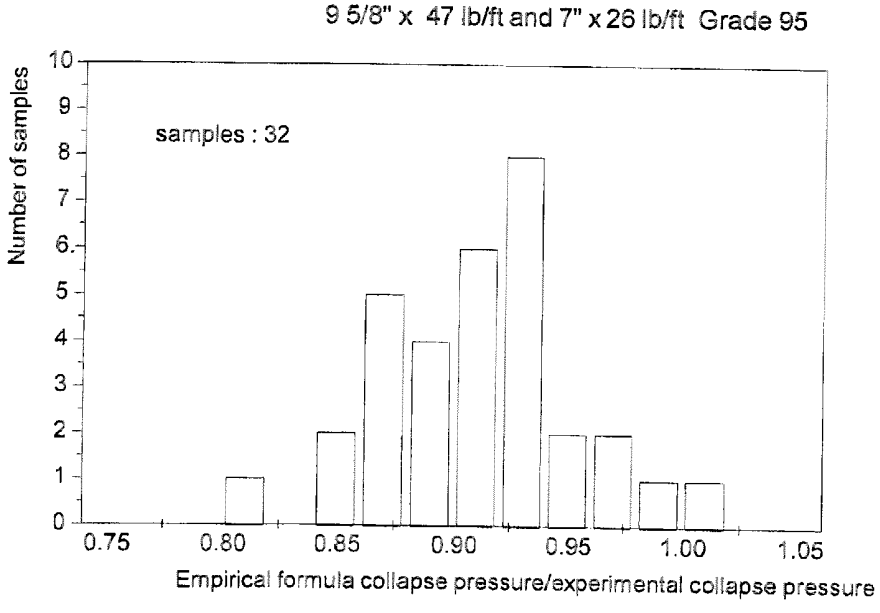

Figure 15.
Analysis of an empirical formula

6. Conclusions

From the experimental and numerical analyses that we publish in this paper we extract some relevant conclusions regarding the external collapse pressure of steel pipes:

- A 2D geometrical description is not enough to characterize the pipe regarding its external collapse pressure. Neither the 2D finite element models nor Tamano's empirical formula, also built on a bidimensional geometrical description of the pipe geometry, have an accuracy high enough for determining external collapse pressures. Industrial practices have to include 3D geometrical characterizations if a limit collapse pressure is going to be guaranteed for an industrial production.
- Circumferential residual stresses are a fundamental element in the determination of the collapse pressure.
- Using well established experimental/numerical techniques it is possible to characterize a pipe regarding its collapse pressure very accurately. Investigating the statistical distribution in geometrical and material parameters of a pipe production it is possible to predict, using 3D finite element models, its collapse pressure distribution.

References

ADINA Users' Manual 1996, Technical Report ARD 96-5, ADINA R & D, Watertown, MA.

Arbocz, J. and Babcock, C.D. (1969), "The effect of general imperfections on the buckling of cylindrical shell", *ASME, J. Appl. Mechs*, Vol. 36, pp. 28-38.

Arbocz, J. and Williams, J.G. (1977), "Imperfection surveys of a 10-ft diameter shell structure", *AIAA Journal*, Vol. 15, pp. 949-56.

Bathe, K.J. (1996), *Finite Element Procedures*, Prentice-Hall, Upper Saddle River, NJ.

Bathe, K.J. and Dvorkin, E.N. (1985), "A four-node plate bending element based on Mindlin/Reissner plate theory and a mixed interpolation", *Int. J. Numer. Meth. Engng*, Vol. 22, pp. 367-83.

Bathe, K.J. and Dvorkin, E.N. (1986), "A formulation of general shell elements – the use of mixed interpolation of tensorial components", *Int. J. Numer. Meth. Engng*, Vol. 22, pp. 697-722.

Brigham, E.O. (1988), *The Fast Fourier Transform and its Applications*, Prentice-Hall, Englewood Cliffs, NJ.

Brush, D.O. and Almroth, B.O. (1975), *Buckling of Bars, Plates and Shells*, McGraw-Hill, New York, NY.

Bull. 5C3 (1994), *Bulletin on Formulas and Calculations for Casing, Tubing, Drill Pipe and Line Pipe Properties*, 6th ed., API.

Clinedinst, W.O. (1977), "Analysis of collapse test data and development of new collapse resistance formulas", Technical report. Report to the API Task Group on Performance Properties.

Corona, E. and Kyriakides, S. (1987), "An unusual mode of collapse of tubes under combined bending and pressure", *ASME, J. Pressure Vessel Technol.*, Vol. 109, pp. 302-04.

Dvorkin, E.N. and Assanelli, A.P. (1989), "Elasto-plastic analysis using a quadrilateral 2-D element based on mixed interpolation of tensorial components", in Owen, D.R.J. *et al.* (Eds) *Proc. 2nd International Conference on Computational Plasticity*.

Dvorkin, E.N. and Bathe, K.J. (1984), "A continuum mechanics based four-node shell element for general non-linear analysis", *Engng Computations*, Vol. 1, pp. 77-88.

Dvorkin, E.N. and Vassolo, S.I. (1989), "A quadrilateral 2-D finite element based on mixed interpolation of tensorial components", *Engng Computations*, Vol. 6, pp. 217-24.

Dvorkin, E.N., Assanelli, A.P. and Toscano, R.G. (1996), "Performance of the QMITC element in two-dimensional elasto-plastic analyses", *Comp. Struct.*, Vol. 58, pp. 1099-129.

Fowler, J.R., Hormberg, B. and Katsounas, A. (1990), "Large scale collapse testing", Technical report, SES Report prepared for the Offshore Supervisory Committee, American Gas Association.

Fowler, J.R., Klementich, E.F. and Chappell, J.F. (1983), "Analysis and testing of factors affecting collapse performance of casing", *ASME J. Energy Res. Tech.*, Vol. 105, pp. 574-9.

Heise, O. and Esztergar, E.P. (1970), "Elastoplastic collapse under external pressure", *ASME, J. Engng for Industry*, Vol. 92, pp. 735-42.

Hill, R. (1971), *The Mathematical Theory of Plasticity*, Oxford University Press, New York, NY.

Kanda, M., Yazaki, Y., Yamamoto, K., Higashiyama, H., Sato, T., Inoue, T., Murata, T.H.H.M. and Yanagimoto, S. (1983), "Development of nt-series oil-country tubular good", *Nippon Steel Technical Report*, Vol. 21, pp. 247-62.

Krug, G. (1983), "Testing of casing under extreme loads", PhD thesis, Institute of Petroleum Engineering, Technische Universität, Clausthal.

Marlow, R.S. (1982), "Collapse performance of hc-95 casing", Technical report, Report for the API PRAC Project No. 80-30.

Mimura, H., Tamano, T. and Mimaki, T. (1987), "Finite element analysis of collapse strength of casing", *Nippon Steel Technical Report*, Vol. 34, pp. 62-9.

Press, W.H., Flannery, B.P., Teukolsky, S.A. and Veherling, W.T. (1986), *Numerical Recipes*, Cambridge University Press, Cambridge.

Shunmugam, M.S. (1991), "Criteria for computer-aided form evaluation", *ASME, J. Engng for Industry*, Vol. 113, pp. 233-8.

Tamano, T., Mimaki, T. and Yaganimoto, S. (1983), "A new empirical formula for collapse resistance of commercial casing", *ASME, Proc. 2nd Int. Offshore Mechanics and Arctic Engineering Symposium*, Houston, pp. 489-95.

Timoshenko, S.P. and Gere, J.M. (1961), *Theory of Elastic Stability*, McGraw-Hill.

Tokimasa, K. and Tanaka, K. (n.d.), "FEM analysis of the collapse strength of a tube", *ASME Paper 84-PVP-104.*.

Tomita, Y. and Shindo, A. (1982), "On the bifurcation and post-bifurcation behavior of thick circular elastic-plastic tubes under lateral pressure", *Comput. Methods Appl. Mech. Engrg*, Vol. 35, pp. 207-19.

Yeh, M.K. and Kyriakides, S. (1988), "Collapse of deepwater pipelines", *ASME J. Energy Res. Tech.*, Vol. 110, pp. 1-11.

Appendix. Algorithm to process the data acquired with the imperfections measuring system

The data are acquired along a spiral path; however, in subsequent analyses we will consider that the points corresponding to a turn are located on a planar section, at an axial distance z_k from an arbitrary origin. As the pitch of the spiral is less than half of the typical wall thickness under analysis, this assumption is valid for the purpose of modelling the collapse test. The data are fitted to a perfect circle (of unknown center and radius) through a least squares method (Yeh and Kyriakides, 1988). This approach is consistent with the subsequent Fourier decomposition (Figure A1).

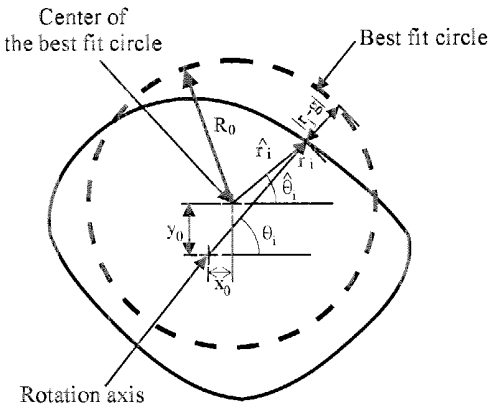

Figure A1.
Algorithm to process the data acquired with the LVDT

Input data:

r_j: radial distance from the rotation axis to the external surface, jth data point.

q_j: total turns corresponding to the jth data point, measured from an arbitrary defined zero.

Algorithm

1. *Initial data reduction.* We can define:

$$k = \text{int}(q_j)$$

the kth turn. For this turn we have

$$z_k = \Delta z \ \text{int}(q_j)$$
$$\theta_i^k = 2\ \pi\ (q_j - \text{int}(q_j))$$
$$r_i^k = r_j$$

where $i = 1$ for the first j which satisfies $(q_j - \text{int}(q_j)) > 0$ (indication of a new turn). Δz indicates the axial advance per turn. The number of data points per turn is not constant.

2. *Fit to best circle.* For the kth section we can define a "best-fit circle", with radius R_0 and with its center located at (x_0,y_0) in a Cartesian system, contained in the section plane and with its origin at the section rotation center. The superindex k in θ_i^k and r_i^k is omitted. For determining R_0,x_0 and y_0 we solve the following minimization problem:

$$(R_0, x_0, y_0) = \arg[\min E_2(R_0, x_0, y_0)]$$
$$E_2 = \sum_i [r_i - g(\theta_i, R_0, x_0, y_0)]^2$$

$$g(\theta_i, R_0, x_0, y_0) = (x_0\ \cos\ \theta_i + y_0\ \sin\ \theta_i) + \sqrt{R_0^2 - (x_0\ \sin\ \theta_i - y_0\ \cos\ \theta_i)^2}$$

To solve the above non-linear minimization problem we apply the Levemberg-Marquard method (Press *et al.*, 1986), using as first trial a simplified (linearized) solution in which the expression for g reduces to (Shunmugam, 1991):

$$g_{lin}(\theta_i, R_0, x_0, y_0) = (x_0\ \cos\ \theta_i + y_0\ \sin\ \theta_i) + R_0$$

3. *Data reduction to the new center.* Once the center of the "best-fit circle" is determined we reduce the acquired data to it,

$$\hat{x}_i = r_i \cos\theta_i - x_0 \quad ; \quad \hat{y}_i = r_i \sin\theta_i - y_0$$

$$\hat{r}_i = \sqrt{\hat{x}_i^2 + \hat{y}_i^2} \quad ; \quad \hat{\theta}_i = \tan^{-1}\left(\frac{\hat{y}_i}{\hat{x}_i}\right)$$

4. Fourier transform. We expand using a discrete Fourier transform

$$\hat{a}_j = \frac{1}{\pi}\sum_{k=1}^{M}\left[\hat{r}_k \cos\left(j\,\hat{\theta}_k\right)\Delta\hat{\theta}_k\right]$$

$$\hat{b}_j = \frac{1}{\pi}\sum_{k=1}^{M}\left[\hat{r}_k \sin\left(j\,\hat{\theta}_k\right)\Delta\hat{\theta}_k\right]$$

where M is the number of samples taken in each turn (360 on average).

5. Shape reconstruction.

$$\hat{r}(\theta) = R_0 + \sum_{j=1}^{N}\left[\hat{a}_j \cos(j\,\theta) + \hat{b}_j \sin(j\,\theta)\right]$$

where N is the number of modes used in the reconstruction of the shape. Sampling theorems (Brigham, 1988) put a limit on the maximum value of N that can be used (in our case $N < M/2 \cong 180$). However, for practical applications in collapse calculations, N is typically lower than 20. For practical purposes we define the amplitude of the j mode of the Fourier decomposition as:

$$A_j = \sqrt{\hat{a}_j^2 + \hat{b}_j^2}.$$